ЖУРНАЛ СТРУКТУРНОЙ ХИМИИ

2015. Том 56, № 8 *Декабрь* *С. 1522 – 1531*

UDC 541.49:546.93:541.67

THEORETICAL VIEW ON STRUCTURE, CHEMICAL REACTIVITY, AROMATICITY AND ^{14}N NQR PARAMETERS OF IRIDAPYRIDINE ISOMERS

R. Ghiasi, E. Amini

Department of Chemistry, Faculty of Basic Science, East Tehran Branch, Islamic Azad University, Qiam Dasht, Tehran, Iran
E-mail: rezaghiasi1353@yahoo.com, rghiasi@iauet.ac.ir

Received October, 22, 2014

Using quantum chemical calculations, we report structures, energetics, natural bond analysis, aromaticity and ^{14}N NQR parameters of the irdidapyridine isomers. The MPW1PW91, PBEPBE and PBE1PBE calculations indicate the most stability for *meta*-isomer. Global electrophilicity index shows that iridapyridines are stronger electrophile rather than pyridine. Local reactivity descriptors as Fukui functions (f_k^+, f_k^-), local softnesses (s_k^+, s_k^-) and electrophilicity indices (ω_k^+, ω_k^-) analyses are performed to find out the reactive sites within molecules. Nucleus-independent chemical shift (NICS) has been evaluated to understand the aromaticity. Also, changes in ^{14}N NQR parameters of the molecules are studied.

DOI: 10.15372/JSC20150802

K e y w o r d s: iridapyridine, frontier orbital analysis, natural bond orbital (NBO) analysis, ^{14}N NQR parameters, nucleus independent chemical shift (NICS).

INTRODUCTION

Metallacyclic aromatic compounds with transition metals are a subject of great attention, because they combine properties of both aromatic organic and organometallic compounds. For example, metallabenzenes are six-membered metallacycles analogous to benzene in which one CH unit has been replaced by an isolobal transition-metal fragment [ML_n]. A significant number of papers have appeared that address synthesis and properties of metallabenzenes [1—6]. For example, a transition metal incorporated into stable metallabenzene complexes is iridium. Synthesis of a series of iridabenzenes has been reported [1—10]. In contrast to the situation with simple metallabenzenes, where there is by now an extensive amount of synthetic, structural, spectral, computational, and reactivity data available [1—3, 11—15], examples of heterocyclic ring metallabenzenes are scarce [16]. For example, synthesis and properties of with metallabenzofuran [17, 18], metallabenzothiophene [18], metallabenzothiazolium [19], metallabenzothiazole [20], and metallabenzoxazole [20] have been reported.

From experimental and theoretical examinations one sees that the actual experimental knowledge concerning hetero-iridabenzenes is still relatively limited [21—23]. The key difference between aromatic metallabenznes and their usual aromatic kin is that π-bonding in the former involves metal *d*-orbitals. The substitution of one atom of the ring in an aromatic organic molecule by an isoelectronic inorganic fragment of a similar shape and energy in their respective frontier orbitals can be illustrated by the isolobal analogy [24, 25].

In the present study, the geometries, aromaticity, chemical reactivity parameters and ^{14}N NQR parameters of iridapyridine and its isomers have been calculated. The NQR spectroscopy can supply a

helpful method to study the details of electronic environment around the nitrogen. Also, natural bond orbital analysis (NBO) provides a detailed insight into the electronic structure.

COMPUTATIONAL METHODS

All calculations were carried out with the Gaussian 09 program suite [26]. The calculations of systems contain C, N, H and P described by the standard 6-311G(*d,p*) basis set [27—30]. For Ir element standard LANL2DZ basis set [31—33] was used with effective core potential (ECP) of Wadt and Hay pseudopotential [31] with a double-ξ valence from LANL2DZ. Also, the aug-cc-pVDZ-PP basis set and effective core potential were used for the Ir atom, for studying of basis set and ECP on the stability of the isomers [34]. Geometry optimization was performed with Modified Perdew-Wang Exchange and Correlation (MPW1PW91) [35]. The results of calculations show that MPW1PW91 functional gives better results than B3LYP [36—39]. Hybrid functional PBE1PBE [40] and PBEPBE [41] methods were used for studying stability of the isomers. Vibrational analysis was performed at each stationary point found, in order to confirm its identity as an energy minimum.

The population analysis has also been performed by the natural bond orbital method [42] using NBO program [43] under Gaussian 2003 program package.

The nucleus-independent chemical shift (NICS) index, based on the magnetic criterion of aromaticity, is probably the most widely used probe for quantifidation of the aromaticity [44]. On the other hand, opposing assignments of aromaticity by NICS and other methods have been reported, particularly for inorganic compounds [45—47]. It is defined as the negative value of the absolute magnetic shielding a ghost atom located at the centre of the aromatic ring (NICS(0) [48]), or at *r*, Å above it (*r* = 0.5, 1, 1.5, 2.0 [49]). Negative NICS values denote efficient electron delocalization. We have also calculated nuclear independent chemical shifts ($NICS_{zz}$) to probe the aromaticity [50, 51]. The $NICS(1)_{zz}$ is the *zz* component of the shielding tensor. The NICS values were calculated using the Gauge independent atomic orbital (GIAO) [52] method with the same procedure and basis sets for optimization.

The electrostatic interaction of a nuclear electric quadrupole moment and the electron charge cloud surrounding the nucleus can give rise to the observation of pure NQR [53]. The Hamiltonian of this interaction is given [54]:

$$H_Q = \frac{e^2 Q q_{zz}}{4I(2I-1)}[3I_x^2 - I^2 + \frac{\eta}{2}(I_+^2 + I_-^2)], \quad (1)$$

where all *I*s in the denominator are scalar values, while all *I*s in the square brackets are operators [55]. Quantum chemical calculations yield principal components of the EFG tensor, q_{ii}, in atomic units (1 au = 9.717365×10^2 V·m^{-2}), with $|q_{zz}| \geq |q_{yy}| \geq |q_{xx}|$. q_{xx}, q_{yy} and q_{zz} are the components of EFG in the directions of *x*, *y* and *z*, respectively. The calculated q_{ii} values were used to obtain the nuclear quadrupole coupling constants, χ_{ii}:

$$\chi_{ii}(\text{MHz}) = \frac{e^2 Q q_{ii}}{h}, \qquad i = x, y, z, \quad (2)$$

where *Q* is the nuclear quadrupole moment of the ^{14}N nucleus. The standard values of quadrupole moment, *Q*, reported by Pyykkö [56] were used in Eq. (1), $Q(^{14}\text{N}) = 20.44$ mb. Often experimental NQR parameters are reported as the nuclear quadrupole coupling constant, and have the unit of frequency:

$$QCC = \chi(\text{MHz}) = \frac{e^2 Q q_{zz}}{h}. \quad (3)$$

Asymmetry parameters (η_Q) are defined as:

$$\eta_Q = \left|\frac{(q_{yy} - q_{xx})}{q_{zz}}\right|, \qquad 0 \leq \eta_Q \leq 1, \quad (4)$$

since it measures the deviation of the field gradient tensor from axial symmetry.

For a nucleus of unit spin (such as ^{14}N), we have three energy levels, so we get three nuclear quadrupole resonance frequencies [54]:

$$\upsilon_+ = \frac{3}{4}\chi_{zz}(1+\frac{\eta}{3}), \tag{5}$$

$$\upsilon_- = \frac{3}{4}\chi_{zz}(1-\frac{\eta}{3}), \tag{6}$$

$$\upsilon_0 = \frac{3}{4}\chi_{zz}\,\eta. \tag{7}$$

The quadrupole coupling constant (χ_{zz}) and asymmetry parameter (η) are usually calculated from the nuclear quadrupole frequencies as follows:

$$\chi_{zz} = \frac{2(\upsilon_+ + \upsilon_-)}{3}, \tag{8}$$

$$\eta = \frac{3(\upsilon_+ - \upsilon_-)}{(\upsilon_+ + \upsilon_-)}. \tag{9}$$

RESULTS AND DISCUSSION

Energetics. Iridabenzene and three isomers of iridapyridines and their arbitrary numbering are presented in Fig. 1. Absolute energies and relative energies (ΔE) of iridabenzene and iridapyridine isomers have calculated in four levels of theory and gathered in Table 1. We can see that the *meta-isomer* has the most stability at the studied levels of theory. Therefore, iridium appears to prefer the soft carbon atom, which is compatible with hard soft acid-base (HSAB) principle [57].

Thermodynamic parameters. Free energies, enthalpies, zero-point correction, relative free energies, and relative enthalpies of title molecules were calculated at four levels of theory and tabulated in Table 1. These values show that addition of zero point energy (ZPE) does not affect the order of relative stabilities.

Geometric parameters. The calculated bond lengths are listed in Fig. 1. According to the theoretical results, three phosphine phosphorous, P_a, P_b, $P_{b'}$, and two 1 and 5 atoms form a square pyramidal environment around iridium.

Ir—C and Ir—N bonds. For analysis of these bonds, the model complexes [$Ir(CH_3)(=CH_2)\times$ $\times(PH_3)_3$] were optimized with MPW1PW91 method and the same basis sets were used for the iridabenzene and iridapyridines. The Ir—C bond length is slightly shorter than that for calculated Ir—C single bond (2.149 Å), but longer than that calculated Ir—C double bond (1.892 Å). The bond distance demonstrate the delocalization of bonding, a typical feature of aromatic molecules.

CC and CN bonds. Analysis of CC bond lengths reveals these bonds are intermediate between normal single and double bonds, compared with 1.324 Å, 1.522 Å, 1.457 Å, and 1.262 Å, in C_2H_4, C_2H_6,

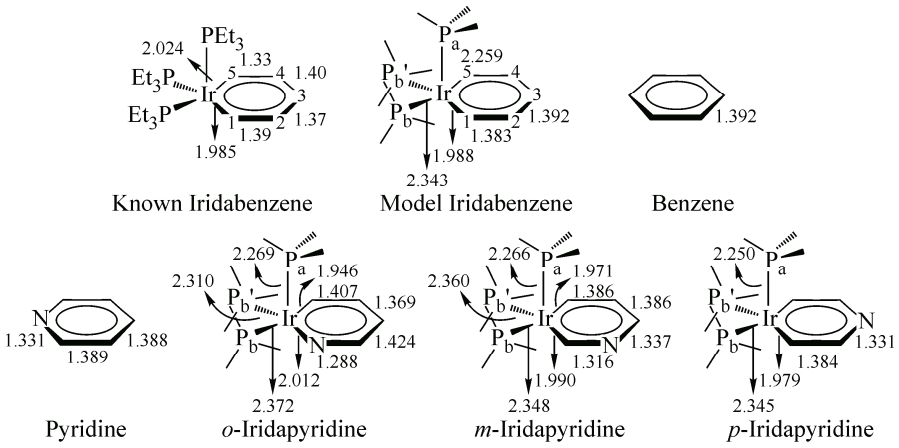

Fig. 1. Structure and bond lengths of synthesized iridabenzene, model iridabenzene, benzene, pyridine and iridapyridine isomers with MPW1PW91 method, 6-311G** and LANL2DZ basis sets for non metal and metal elements, respectively

Table 1

Absolute energies (Hartree), *relative energies* (kcal/mol), *free energies* (Hartree), *enthalpies* (Hartree), *zero-point correction* (Hartree), *relative free energies* (kcal/mol), *and relative enthalpies* (kcal/mol) *values of iridabenzene and three isomers of iridapyridines*

L	*E*	Zero-point correction	*E*+ZPE	Δ*E*	ΔE^{zpe}	*G*	*H*	Δ*G*	Δ*H*
Method 1*: MPW1PW91									
IB	–1327.805	0.167	–1327.64	—	—	–1327.680	–1327.623	—	—
o-Ipy	–1343.840	0.155	–1343.68	4.61	4.45	–1343.727	–1343.669	4.34	4.50
m-Ipy	–1343.847	0.155	–1343.69	0.00	0.00	–1343.734	–1343.677	0.00	0.00
p-Ipy	–1343.840	0.156	–1343.68	4.05	4.34	–1343.727	–1343.670	4.45	4.24
Method 2*: PBEPBE									
IB	–1327.0485	0.161	–1326.89	—	—	–1326.930	–1326.872	—	—
o-Ipy	–1343.0872	0.148	–1342.94	3.04	2.93	–1342.981	–1342.923	2.99	2.94
m-Ipy	–1343.0920	0.149	–1342.94	0.00	0.00	–1342.986	–1342.928	0.00	0.00
p-Ipy	–1343.0851	0.149	–1342.94	4.33	4.66	–1342.978	–1342.921	4.80	4.52
Method 3*: PBE1PBE									
IB	–1327.117	0.167	–1326.95	—	—	–1326.992	–1326.935	—	—
o-Ipy	–1343.144	0.155	–1342.99	4.90	4.73	–1343.032	–1342.974	4.68	4.78
m-Ipy	–1343.152	0.155	–1343.00	0.00	0.00	–1343.039	–1342.982	0.00	0.00
p-Ipy	–1343.145	0.155	–1342.99	4.03	4.33	–1343.032	–1342.975	4.45	4.22
Method 4**: MPW1PW91									
IB	–1327.679	0.167	–1327.51	—	—	–1327.554	–1327.497	—	—
o-Ipy	–1343.717	0.155	–1343.56	2.65	2.43	–1343.605	–1343.547	2.24	2.50
m-Ipy	–1343.721	0.155	–1343.57	0.00	0.00	–1343.608	–1343.551	0.00	0.00
p-Ipy	–1343.715	0.155	–1343.56	3.89	4.03	–1343.602	–1343.545	3.87	3.98

*6-311G** and LANL2DZ basis sets for non-metal and metal elements, respectively.
6-311G and aug-cc-pVDZ-PP basis sets for non metal and metal elements, respectively.

H_3CNH_2, and H_2CNH respectively, calculated by MPW1PW91 method and with 6-311G(*d*,*p*) basis set. These data demonstrate the delocalization of bonding, with character of aromatic molecules.

Ir—P bonds. Ir—P bond distances values are gathered in Fig. 1. These values indicate that the Ir—P basal bonds are longer than the Ir—P apical bonds.

The predicted values are close to the experimental values [58]. The minor differences may due to the fact that the theoretical calculations were applied to the isolated molecule in gas phase, and the experimental results were applied to the molecule in the solid state. The calculated geometric parameters represent a good approximation and can be used as foundation to calculate the other parameters.

Table 2

Frontier orbital energies (a.u.), *frontier orbitals gap* (eV), *hardness* (eV), *softness* (1/eV), *chemical potential* (eV) *and electrophilicity* (eV) *values of benzene*, *pyridine*, *iridabenzene and three isomers of iridapyridines calculated with* MPW1PW91 *method*, 6-311G** *and* LANL2DZ *basis sets for non-metal and metal elements*, *respectively*

Molecule	HOMO	LUMO	Δ*E*	η	*S*	μ	ω
Benzene	–0.267	–0.003	7.18	3.59	0.28	–3.66	1.87
IB	–0.184	–0.048	3.69	1.85	0.54	–3.15	2.69
Pyridine	–0.271	–0.026	6.66	3.33	0.30	–4.05	2.46
o-Irpy	–0.192	–0.058	3.65	1.83	0.55	–3.40	3.16
m-Irpy	–0.190	–0.055	3.69	1.85	0.54	–3.33	3.00
p-Irpy	–0.200	–0.063	3.73	1.87	0.54	–3.57	3.42

Table 3

Selected nucleophilic reactivity descriptors (f_k^-, s_k^-, ω_k^-), *selected electrophilic reactivity descriptors* (f_k^+, s_k^+, ω_k^+) *of three isomers of iridapyridines obtained with* MPW1PW91 *method*, 6-311G** *and* LANL2DZ *basis sets for non-metal and metal elements*, *respectively*

	Ir	1	2	3	4	5
			f^+			
o-Irpy	0.7384	–0.2871	0.0561	–0.2066	0.0286	–0.6152
m-Irpy	0.8329	–0.7161	0.4313	–0.2742	0.1979	–0.7462
p-Irpy	0.7960	–0.5868	0.0029	0.0801	–0.0039	–0.5821
			f^-			
o-Irpy	–0.6437	0.3275	–0.0200	0.2593	0.0280	0.5849
m-Irpy	–0.8856	0.7378	–0.3347	0.4008	–0.1585	0.7431
p-Irpy	–0.8578	0.5830	0.0652	0.0547	0.0660	0.5826
			f^0			
o-Irpy	0.0947	0.0403	0.0361	0.0527	0.0567	–0.0304
m-Irpy	–0.0527	0.0217	0.0966	0.1266	0.0394	–0.0031
p-Irpy	–0.0619	–0.0038	0.0681	0.1348	0.0621	0.0006
			ω^+			
o-Irpy	3.1567	2.3308	–0.9064	0.1770	–0.6523	0.0903
m-Irpy	3.0025	2.5007	–2.1500	1.2950	–0.8231	0.5943
p-Irpy	3.4156	2.7188	–2.0041	0.0099	0.2736	–0.0133
			ω^-			
o-Irpy	–2.0318	1.0338	–0.0630	0.8187	0.0885	1.8463
m-Irpy	–2.6589	2.2152	–1.0049	1.2034	–0.4759	2.2313
p-Irpy	–2.9301	1.9913	0.2227	0.1867	0.2254	1.9901
			ω^0			
o-Irpy	0.2990	0.1274	0.1139	0.1664	0.1789	–0.0958
m-Irpy	–0.1582	0.0652	0.2901	0.3803	0.1184	–0.0093
p-Irpy	–0.2113	–0.0129	0.2326	0.4603	0.2120	0.0019
			s^+			
o-Irpy	0.4042	–0.1572	0.0307	–0.1131	0.0157	–0.3368
m-Irpy	0.4509	–0.3877	0.2335	–0.1484	0.1072	–0.4040
p-Irpy	0.4263	–0.3142	0.0016	0.0429	–0.0021	–0.3117
			s^-			
o-Irpy	–0.3524	0.1793	–0.0109	0.1420	0.0154	0.3202
m-Irpy	–0.4794	0.3994	–0.1812	0.2170	–0.0858	0.4023
p-Irpy	–0.4594	0.3122	0.0349	0.0293	0.0353	0.3120
			s^0			
o-Irpy	0.0519	0.0221	0.0198	0.0289	0.0310	–0.0166
m-Irpy	–0.0285	0.0118	0.0523	0.0686	0.0214	–0.0017
p-Irpy	–0.0331	–0.0020	0.0365	0.0722	0.0332	0.0003

Chemical reactivity. Global reactivity descriptors. Global reactivity descriptors [59—63] electronegativity (χ), chemical potential (μ), global hardness (η), global softness (S), and electrophilicity index (ω) were determined on the basis of Koopman′s theorem [64]. Frontier orbital energies, frontier orbitals gap, hardness, softness, chemical potential and electrophilicity values are listed in Table 2. These values indicate the most hardness and electrophilicity and lowest chemical potential for *para*-isomer of iridapyridine.

Local reactivity descriptors. Selected nucleophilic reactivity descriptors f_k^-, s_k^-, ω_k^- for molecules, obtained with Mulliken atomic charges, are given in Table 3. In iridapyridine, the maximum values of the local nucleophilic reactivity descriptors f_k^-, s_k^-, ω_k^- at C5 atom indicate that this site is prone to electrophilic attack.

Selected electrophilic reactivity descriptors f_k^+, s_k^+, ω_k^+ [65], are given in Table 3. The maximum values of local electrophilic reactivity descriptors f_k^+, s_k^+, ω_k^+ at Ir atom indicate that this site is more prone to nucleophilic attack.

Nucleus independent chemical shift analyses (NICS). NICS is an easy and efficient criterion to identify aromatic nature. A large negative NICS value at the ring center (or inside and above the molecular plane) implies the presence of diamagnetic ring currents. As shown in Table 4, all computed NICS(0.0) values at the geometrical center of cycles are in the range of –4.5 ppm to –4.2 ppm, suggesting that such frames are obviously aromatic. In order to further quantify the aromaticity of the molecules, we calculated the NICS values (including NICS(0.5), NICS(1.0), NICS(1.5), and NICS(2.0)) by placing a series of ghost atoms above (by 0.5 Å, 1.0 Å, 1.5 Å, 2.0 Å) the geometrical centers. All these NICS values are mainly attributable to the delo- calized π electron current. The most negative of these values are

Table 4

The NICS *values* (ppm) *for the pyridine*, *iridabenzene and three isomers of iridapyridines obtained with* MPW1PW91 *method*, 6-311G** *and* LANL2DZ *basis sets for non-metal and metal elements*, *respectively*

Parameter	NICS (0.0)	NICS(0.5)	NICS(1.0)	NICS(1.5)	NICS(2.0)	$NICS(0.0)_{zz}$	$NICS(0.5)_{zz}$	$NICS(1.0)_{zz}$	$NICS(1.5)_{zz}$	$NICS(2.0)_{zz}$
Pyridine	–7.57	–10.16	–11.06	–8.22	–5.17	–13.45	–22.74	–29.18	–24.09	–16.74
IrB	–5.33	–7.33	–8.33	–6.8	–4.85	–2.72	–8.66	–16.34	–16.82	–13.04
o-Irpy	–4.54	–6.24	–7.63	–6.5	–4.66	–2.51	–7.73	–15.47	–16.06	–12.77
m-Irpy	–4.22	–6.22	–7.65	–6.34	–4.44	–2.77	–8.12	–15.41	–15.71	–12.22
p-Irpy	–4.52	–6.96	–8.56	–7.08	–4.90	–4.96	–10.55	–17.74	–17.50	–13.42

Table 5

Occupancy of the σ(Ir—P) *orbitals and electron configuration of* Ir *in iridabenzene and irdiapyridine isomers calculated with* MPW1PW91 *method*, 6-311G** *and* LANL2DZ *basis sets for non-metal and metal elements*, *respectively*

Complex	Ir—P_a	Ir—P_b	Ir—$P_{b'}$	Ir configuration
IrB	1.8858	1.9100	1.9902	[core]6*s*(0.47)5*d*(8.47)6*p*(1.37)6*d*(0.02)
o-Irpy	1.8808	1.9070	1.8948	[core]6*s*(0.47)5*d*(8.36)6*p*(1.26)6*d*(0.02)
m-Irpy	1.8893	1.9157	1.9149	[core]6*s*(0.48)5*d*(8.48)6*p*(1.37)6*d*(0.01)
p-Irpy	1.8749	1.9139	1.9087	[core]6*s*(0.47)5*d*(8.44)6*p*(1.35)6*d*(0.01)

1.0 Å above of the ring center. For this reason, aromticity of these iridapyridine isomers increases in the *ortho* < *meta* < *para* row. We also calculated $NICS_{zz}$ to probe aromaticity in studied molecules (Table 4). The $NICS_{zz}$ is large and negative at the 1.5 Å above the ring center, thus providing additional evidence for aromaticity of these molecules.

Natural bond orbital analysis. NBO analysis has provided detailed insight into the nature of electronic conjugation between the bonds in these molecules. According to the NBO results, the electron configuration of Ir in iridabenzene and irdiapyridine isomers is gathered in Table 5. The electron configuration of Ir is: [core] $6s^a5d^b6p^c6d^d7p^e$.

The computed Wiberg bond indices [66] of all molecules are summarized in Table 6. The sum of the Wiberg bond orders in the ring, $\sum BO_R$, takes on values of 7.929, 7.878, and 7.883, respectively, for *ortho*-, *meta*-, and *para*-iridapyridine isomers. For comparison, the corresponding value for pyridine is 8.584. It should be pointed out that, while $\sum BO_R$ is a good indicator of ionic/covalent character, it is not an aromaticity criterion since a hypothetical 1,3,5-cyclohexatriene would have a $\sum BO_R$ value close to 9.00 as well. In short, the *meta* > *para* > *ortho* stability order can be explained as an interplay be tween ionic bonding and aromaticity considerations. We note from the Wiberg indices that bonding in the *ortho*-isomer is more covalent than in *meta*- and *para*-isomers.

Table 6

The computed Wiberg bond indices and their sums for benzene, *pyridine*, *iridabenzene and three isomers of iridapyridines calculated with* MPW1PW91 *method*, 6-311G** *and* LANL2DZ *basis sets for non-metal and metal elements*, *respectively*

Molecule	Ir—1	1—2	2—3	3—4	4—5	5—Ir	$\sum BO_{ring}$
Benzene	1.436	1.436	1.436	1.436	1.436	1.436	8.615
Pyridine	1.427	1.428	1.437	1.437	1.428	1.427	8.584
IrB	1.055	1.505	1.388	1.388	1.505	1.055	7.897
o-Irpy	0.898	1.711	1.230	1.535	1.356	1.200	7.928
m-Irpy	1.047	1.513	1.341	1.424	1.459	1.093	7.877
p-Irpy	1.067	1.485	1.389	1.390	1.484	1.069	7.883

Table 7

Natural orbital occupancy (*number of electrons*, *or "natural population" of the orbital*) *of* Ir—C *and* Ir—N *bonds in iridabenzene and three isomers of iridapyridines calculated with* MPW1PW91 *method*, 6-311G** *and* LANL2DZ *basis sets for non-metal and metal elements*, *respectively*

Molecule	Bond	Occupancy	Hybridation
IrB	Ir—5	1.81345	σ: 0.7858 C5 *sp* 1.78 + 0.6185 Ir *sp* 1.70 *d* 1.53
	Ir—1	1.82018	σ: 0.7761 C1 *sp* 1.85 + 0.6306 Ir *sp* 1.90 *d* 1.99
		1.51401	π: 0.6626 C1 *p* 50.14 + 0.7490 Ir *p* 8.46 *d* 11.74
o-Irpy	Ir—1	1.83813	σ: 0.5521 Ir *sp* 2.18 d 2.27 + 0.8338 N1 *sp* 3.30
	Ir—5	1.82424	σ: 0.7864 C5 *sp* 1.85 + 0.6177 Ir *sp* 1.60
		1.58897	π: 0.6954 C5 *p* 32.84 + 0.7186 Ir *p* 7.57 *d* 10.08
m-Irpy	Ir—1	1.82218	σ: 0.7770 C1 *sp* 1.51 + 0.6295 Ir *sp* 1.72 *d* 1.56
	Ir—5	1.82631	σ: 0.7802 C5 *sp* 1.82 + 0.6256 Ir *sp* 1.83 *d* 1.90
		1.53284	π: 0.6533 C5 *p* 48.62 + 0.7571 Ir *p* 9.29 *d* 13.01
p-Irpy	Ir—1	1.80518	σ: 0.7828 C 1 *sp* 1.81 + 0.6222 Ir *sp* 1.68 *d* 1.51
	Ir—5	1.81908	σ: 0.7749 C5 *sp* 1.84 + 0.6321 Ir *sp* 1.85 *d* 1.93
		1.50877	π: 0.6948 C5 *p* 61.28 + 0.7192 Ir *p* 9.33 *d* 13.12

Table 7 shows calculated natural orbital occupancy (number of electrons, or ″natural population″ of the orbital) and hybridization of Ir—C and Ir—N bonds. It can be noted that for σ(Ir—C) bonding orbital, the maximum occupancy is obtained for the *meta-isomer*. On the other hand, σ(Ir—N) bond orbital occupancy is higher than σ(Ir—C). For all molecules, the *s* and *p* orbitals of carbon and nitrogen and *s*, *p* and *d* orbitals of iridium contribute in the σ_{IrX}-bond formation (X = C, N). On the other hand, the increasing *d*-character on iridium NHO σ(IrX) results in a lengthening of the Ir—X bond.

The most important interaction between ″filled″ (donor) Lewis type NBOs and ″empty″ (acceptor) non-Lewis NBOs is reported in Table 8. This shows that the highest charge transfer energy is BD (2) C5—Ir → BD*(2) C4—N in *para*-isomer. Also, the most important charge transfer interaction of LP(N) is listed in Table 8. As Shown in Table 8, there is a strong interactions between LP(N) and antibonding Ir—N and Ir—C orbitals, respectively, in the *o*-Irpy and *m*-Irpy molecules. This is indicated by a decrease in the population of LP(N).

The results of NBO calculations may also explain the fact that the calculated basal Ir—P bonds are slightly longer than the Ir—P bonds to the apical phosphine groups. The NBO calculations show that the occupancy on σ(Ir—P_{basal}) orbital is larger than σ(Ir—P_{apical}) orbital (Table 5).

Table 8

The second-order perturbation energies E(2) (kcal/mol) *corresponding to the most important charge transfer interactions* (*donor* → *acceptor*) *in the compounds studied*, *and* LP(N) → *acceptor obtained with* MPW1PW91 *method*, 6-311G** *and* LANL2DZ *basis sets for non-metal and metal elements*, *respectively*

Molecule	Donor NBO→acceptor NBO	*E*(2)	*E*(*j*) – *E*(*i*)	*F*(*i*,*j*)	Occupancy
IrB	BD(2) C2—C3 → BD*(2) C1—Ir	30.28	0.25	0.079	—
o-Irpy	BD(2) C5—Ir → BD*(2) C3—C4	21.19	0.26	0.069	1.8826
m-Irpy	BD(2) C3—C4 → BD*(2) C5—Ir	30.53	0.26	0.080	1.8797
p-Irpy	BD(2) C5—Ir → BD*(2) C4—N	34.37	0.23	0.080	1.9158
Pyridine	LP(1) N → BD*(1) C1—C2	9.84	0.93	0.087	1.91831
o-Irpy	LP(1) N → BD*(1) C2—C3	11.49	0.92	0.093	1.88263
m-Irpy	LP(1) N → BD*(1) C1—Ir	11.40	0.67	0.078	1.87968
p-Irpy	LP(1) N → BD*(1) C1—C2	10.43	0.95	0.090	1.91577

Table 9

The calculated NQR *parameters and principal components of the* EFG *tensors for the pyridine and three isomers of iridapyridines*

Molecule	q_{xx}(a. u.)	q_{yy}(a. u.)	q_{zz}(a. u.)	$(e^2Q/h)q_{xx}$	$(e^2Q/h)q_{yy}$	$(e^2Q/h)q_{zz}$	η	υ_+	υ_-	υ_0
Pyridine	–0.352	–0.777	1.129	1.692	3.730	5.422	0.376	4.576	3.557	1.019
o-Irpy	–0.125	–0.909	1.034	0.602	4.365	4.967	0.758	4.666	2.785	1.882
m-Irpy	–0.370	–0.623	0.993	1.777	2.994	4.771	0.255	3.882	3.274	0.608
p-Irpy	–0.332	–0.841	1.173	1.595	4.038	5.632	0.434	4.835	3.613	1.222

^{14}N NQR PARAMETERS

The asymmetry of the charge distributions around nitrogen atoms has been investigated, and interpreted by EFGs. Since the EFG around a nitrogen nucleus is symmetric in N_2 free molecule, the calculated values of NQR parameters for N_2 molecule are $\eta_Q = 0$ and $\nu_Q^{cal} = 4.258$ MHz. The calculated NQR frequencies of the nitrogen atoms in pyridine and iridapyridine isomers in the gas phase are listed in Table 9. The differences between the frequencies of nitrogens in these species can be attributed to the direct participation of the electron pairs of some N atoms during chemical bond formation or diatropic current in the ring.

From the results listed in Table 9, it is obvious that the χ_{zz} values for nitrogen atoms decrease in the row: *p*-Irpy > *o*-Irpy > *m*-Irpy. The electric field gradient around a given nucleus arises from the charge distribution of the surrounding atoms, and the contribution of nonbonding electrons is higher than of bonding electrons. The decreasing q_{zz} and χ_{zz} values are attributed to the contribution of the lone pair electrons of nitrogen into of π bond. Whenever the lone pair electrons of nitrogen participates in the formation of π bond, the q_{zz} and consequently χ_{zz} decrease. This result is compatible with NBO predictions. The occupancy of LP(N) NBO decreases in the row: *p*-Irpy > *o*-Irpy > *m*-Irpy. Decreasing occupancy for LP(N) NBO shows more contribution of the lone pair electrons of nitrogen into π bonding.

CONCLUSIONS

In this paper we have showed that:

1. The most stable isomer of iridapyridines is *meta*-isomer.

2. Structural parameters are compatible with thearomaticity of the rings. Also, these values indicate Ir—P basal bonds are longer than Ir—P apical. The results from NBO calculations explain the fact that the calculated basal Ir—P bonds are slightly longer than the remaining Ir—P bonds to the apical phosphine groups.

3. The global elecrophilicity index of iridapyridines indicates them as strong electrophiles.

4. NICS study showed that diatropic currents exist in the heterocycle rings of all of the three isomers, so these iridapyridines are aromatic.

5. The quadrupole coupling constant values for nitrogen atoms are reduced compared with free N_2 molecule.

The authors are grateful for the financial support of this work by research and technology deputy of east Tehran branch of Islamic Azad University.

REFERENCES

1. *Bleeke J.R.* // Chem. Rev. – 2001. – **101**. – P. 1205 – 1227.
2. *He G., Xia H., Jia G.* // Chin. Sci. Bull. – 2004. – **49**. – P. 1543 – 1553.
3. *Wright L.J.* // J. Chem. Soc., Dalton Trans. – 2006. – P. 1821 – 1827.
4. *Chen J., Jia G.* // Coord. Chem. Rev. – 2013. – **257**. – P. 2491 – 2521.
5. *Ghiasi R.* // Russ. J. Coord. Chem. – 2011. – **37**. – P. 72 – 76.
6. *Jacob V., Landorf C.W., Zakharov L.N., Weakley T.J.R., Haley M.M.* // Organometallics. – 2009. – **28**. – P. 5183 – 5190.

7. *Paneque M., Posadas C.M., Poveda M.L.* // J. Am. Chem. Soc. – 2003. – **125**. – P. 9898 – 9899.
8. *Gilbertson R.D., Lau T.L.S., Lanza S.* // Organometallics. – 2003. – **22**. – P. 3279 – 3289.
9. *Gilbertson R.D., Weakley T.J.R., Haley M.M.* // J. Am. Chem. Soc. – 1999. – **121**. – P. 2597 – 2598.
10. *Gilbertson R.D., Weakley T.J.R., Haley M.M.* // Chem. Eur. J. – 2000. – **6**. – P. 437 – 441.
11. *Landorf C.W., Haley M.M.* // Angew. Chem., Int. Ed. – 2006. – **45**. – P. 3914 – 3936.
12. *Fernandez I., Frenking G.* // Chem. Eur. J. – 2007. – **13**. – P. 5873 – 5884.
13. *Iron M.A., Lucassen A.C.B., Cohen H., van der Boom M.E., Martin J.M.L.* // J. Am. Chem. Soc. – 2004. – **126**. – P. 11699 – 11710.
14. *Rickard C.E.F., Roper W.R., Woodgate S.D., Wright L.J.* // Angew. Chem., Int. Ed. – 2000. – **39**. – P. 750 – 752.
15. *Clark G.R., Johns P.M., Roper W.R., Wright L.J.* // Organometallics. – 2008. – **27**. – P. 451 – 454.
16. *Ghiasi R., Mokarram E.E.* // Russ. J. Coord. Chem. – 2011. – **37**. – P. 463 – 467.
17. *Clark G.R., Johns P.M., Roper W.R., Wright L.J.* // Organometallics. – 2006. – **25**. – P. 1771 – 1177.
18. *Clark G.R., Lu G.-L., Roper W.R., Wright L.J.* // Organometallics. – 2007. – **26**. – P. 2167 – 2177.
19. *Dalebrook A.F., Wright L.J.* // Organometallics. – 2009. – **28**. – P. 5536 – 5540.
20. *Wang T., Li S., Zhang H., Lin R., Han F., Lin Y., Wen T.B., Xia H.* // Angew. Chem., Int. Ed. – 2009. – **48**. – P. 6453 – 6456.
21. *Chen J., Daniels L.M., Angelici R.J.* // J. Am. Chem. Soc. – 1990. – **112**. – P. 199 – 204.
22. *Bianchini C., Meli A., Peruzzini M. et al.* // J. Am. Chem. Soc. – 1993. – **115**. – P. 2731 – 2742.
23. *Bianchini C., Meli A., Peruzzini M. et al.* // J. Am. Chem. Soc. – 1994. – **116**. – P. 4370 – 4381.
24. *Islas R., Poater J., Solà M.* // Organometallics. – 2014. – **33**. – P. 1762 – 1773.
25. *Hoffmann R.* // Angew. Chem., Int. Ed. Engl. – 1982. – **21**. – P. 711 – 724.
26. *Frisch M.J., Trucks G.W., Schlegel H.B., Scuseria G.E., Robb M.A., Cheeseman J.R., Scalman G., Barone V., Mennucci B., Petersson G.A., Nakatsuji H., Caricato M., Li X., Hratchian H.P., Izmaylov A.F., Bloino J., Zheng G., Sonnenberg J.L., Hada M., Ehara M., Toyota K., Fukuda R., Hasegawa J., Ishida M., Nakajima T., Honda Y., Kitao O., Nakai H., Vreven T., Montgomery J.A. Jr., Peralta J.E., Ogliaro F., Bearpark M., Heyd J.J., Brothers E., Kudin K.N., Staroverov V.N., Kobayashi R., Normand J., Raghavachari K., Rendell A., Burant J.C., Iyengar S.S., Tomasi J., Cossi M., Rega N., Millam J.M., Klene M., Knox J.E., Cross J.B., Bakken V., Adamo C., Jaramillo J., Gomperts R., Stratmann R.E., Yazyev O., Austin A.J., Cammi R., Pomelli C., Ochterski J.W., Martin R.L., Morokuma K., Zakrzewski V.G., Voth G.A., Salvador P., Dannenberg J.J., Dapprich S., Daniels A.D., Farkas O., Foresman J.B., Ortiz J.V., Cioslowski J., Fox D.J.* In: Gaussian Inc. – Wallingford, CT, 2009.
27. *Krishnan R., Binkley J.S., Seeger R., Pople J.A.* // J. Chem. Phys. – 1980. – **72**. – P. 650 – 654.
28. *Wachters A.J.H.* // J. Chem. Phys. – 1970. – **52**. – P. 1033.
29. *Hay P.J.* // J. Chem. Phys. – 1977. – **66**. – P. 4377 – 4384.
30. *McLean A.D., Chandler G.S.* // J. Chem. Phys. – 1980. – **72**. – P. 5639 – 5648.
31. *Hay P.J., Wadt W.R.* // J. Chem. Phys. – 1985. – **82**. – P. 299 – 310.
32. *Hay P.J., Wadt W.R.* // J. Chem. Phys. – 1985. – **82**. – P. 284 – 298.
33. *Schaefer A., Horn H., Ahlrichs R.* // J. Chem. Phys. – 1992. – **97**. – P. 2571 – 2577.
34. *Figgen D., Peterson K.A., Dolg M., Stoll H.* // J. Chem. Phys. – 2009. – **130**. – P. 164108.
35. *Adamo C., Barone V.* // J. Chem. Phys. – 1998. – **108**. – P. 664 – 675.
36. *Porembski J.P.C.A.M., Weisshaar J.C.* // J. Phys. Chem. A. – 2001. – **105**. – P. 4851.
37. *Porembski M., Weisshaar J.C.* // J. Phys. Chem. A. – 2001. – **105**. – P. 6655 – 6667.
38. *Zhang Y., Guo Z., You X.-Z.* // J. Am. Chem. Soc. – 2001. – **123**. – P. 9378 – 9387.
39. *Dunbar R.C.* // J. Phys. Chem. A. – 2002. – **106**. – P. 7328 – 7337.
40. *Adamo C., Barone V.* // J. Chem. Phys. – 1999. – **110**. – P. 6158 – 6170.
41. *Perdew J.P., Burke K., Ernzerhof M.* // Phys. Rev. Lett. – 1996. – **77**. – P. 3865 – 3868.
42. *Reed A.E., Curtiss L.A., Weinhold F.* // Chem. Rev. – 1988. – **88**. – P. 899 – 926.
43. *Glendening E.D., Reed A.E., Carpenter J.E., Weinhold F.* In: Gaussian Inc. – Pittsburg, PA, 2003.
44. *Chen Z., Wannere C.S., Corminboeuf C., Puchta R., Schleyer P.v.R.* // Chem. Rev. – 2005. – **105**. – P. 3842 – 3888.
45. *Torres-Vega J.J., V-Espinal A., Caballero J., Valenzuela M.L., A-Thon L., Osorio E., Tiznado W.* // Inorg. Chem. – 2014. – **53**. – P. 3579 – 3585.
46. *Islas R., M-Guajardo G., Jiménez-Halla J.O.C., Sola M., Merino G.* // J. Chem. Theory Comput. – 2010. – **6**. – P. 1131 – 1135.
47. *Torres J.J., Islas R., Osorio E., Harrison J.G., Tiznado W., Merino G.* // J. Phys. Chem. A. – 2013. – **117**. – P. 5529 – 5533.

48. *Schleyer P.v.R., Marker C., Dransfeld A., Jiao H., Hommes N.J.R.V*. // J. Am. Chem. Soc. – 1996. – **118**. – P. 6317 – 6318.
49. *Schleyer P.v.R., Monohar M., Wang Z., Kiran B., Jiao H., Puchta R., Hommes N.J.R.V*. // Org. Lett. – 2001. – **3**. – P. 2465 – 2468.
50. *Corminboeuf C., Heine T., Seifert G., Schleyer P.v.R., Weber J*. // Phys. Chem. Chem. Phys. – 2004. – **6**. – P. 273 – 276.
51. *Fallah-Bagher-Shaidaei H., Wannere C.S., Corminboeuf C., Puchta R., Schleyer P.v.R*. // Org. Lett. – 2006. – **8**. – P. 863 – 866.
52. *Wolinski K., Hinton J.F., Pulay P*. // J. Am. Chem. Soc. – 1990. – **112**. – P. 8251 – 8260.
53. *Graybeal J.D*. Molecular Spectroscopy. – McGraw-Hill, 1988.
54. *Seliger J*. Nuclear Quadrupole Resonance, Theory — Encyclopedia of Spectroscopy and Spectrometry. – Academic Press, 2000.
55. *Slichter C.P*. Principles of Magnetic Resonance. – 3rd ed. – Heidelberg: Springer-Verlag, 1990.
56. *Pyykko P*. // Mol. Phys. – 2001. – **99**. – P. 1617 – 1629.
57. *Huheey J.E., Keiter E.A., Keiter R.L*. Inorganic Chemistry, Principles of structure and Reactivity. – 4th ed. – New York: Harper and Row, 1994.
58. *Bleeke J. R., Xie Y.-F., Peng W.-J., Chiang M*. // J. Am. Chem. Soc. – 1989. – **111**. – P. 4118 – 4120.
59. *Pearson R.G*. // J. Org. Chem. – 1989. – **54**. – P. 1430 – 1432.
60. *Parr R.G., Pearson R.G*. // J. Am. Chem. Soc. – 1983. – **105**. – P. 7512 – 7516.
61. *Geerling P., Proft F.D., Langenaeker W*. // Chem. Rev. – 2003. – **103**. – P. 1793 – 1874.
62. *Parr R.G., Szentpály L.v., Liu S*. // J. Am. Chem. Soc. – 1999. – **121**. – P. 1922 – 1924.
63. *Chattaraj P.K., Sarkar U., Roy D.R*. // Chem. Rev. – 2006. – **106**. – P. 2065 – 2091.
64. *Parr R.G., Yang W*. Density Functional Theory of Atoms and Molecules. – Oxford, New York: Oxford University Press, 1989.
65. *Yang W., Mortier W.J*. // J. Am. Chem. Soc. – 1986. – **108**. – P. 5708 – 5711.
66. *Wiberg K.B*. // Tetrahedron. – 1968. – **24**. – P. 1083.